Development of Low Noise, Back-Side Illuminated Silicon Photodiode Arrays [1]

S.E. Holland *Member, IEEE*, N.W. Wang *Member, IEEE*, and W.W. Moses *Senior Member, IEEE*
Lawrence Berkeley National Laboratory
University of California
Berkeley, CA 94720

Abstract

We have developed low noise, high quantum efficiency photodiode arrays for use with positron-emission tomography (PET). A fabrication process developed for high-energy physics detectors was modified to allow for back-side illumination. A back-side contact consisting of a thin (10 nm) n^+ polysilicon layer covered by an indium tin oxide (ITO) antireflection coating (57 nm) results in $>$ 70% quantum efficiency over the wavelength range of 400–1000 nm. The photodiodes are operated fully depleted (300 μm thick) resulting in a measured capacitance of 3.2 pF and typical leakage currents of 20–50 pA for a 3 mm square element. At room temperature the noise measured at a shaping time of 4 μs is 140 e^- rms. When coupled to a CsI(Tl) scintillator and excited with 141 keV gamma rays, the energy resolution is 12% fwhm.

I. Introduction

The motivation for this work is to develop silicon photodiode arrays suitable for use in positron-emission tomography (PET). The photodiodes, in conjunction with photomultiplier tubes, allow for the determination of both the crystal of interaction and the depth of interaction within an individual crystal for the 511 keV photons [1]. Measurement of the depth of interaction allows for the elimination of the radial elongation artifact which is a significant problem in high-resolution PET [1, 2].

This application requires close-packed arrays of photodiodes segmented to match the size of the scintillator crystals. Due to the small signal levels generated by 511 keV interactions in scintillator crystals, e.g. as low as 700 photons, the photodiodes must have low noise, implying minimal leakage current and capacitance.

For this application, it is desirable to illuminate the photodiodes from the back side, i.e. the unpatterned side. This allows for illumination through a uniform optical window which eliminates dead areas in the device perimeter due to the metallization used to contact the photodiode. The arrays are read out with a custom integrated circuit [3], and back illumination also simplifies the mechanical interface between the readout electronics and the photodiodes. The noise can be reduced for a back-illuminated device due to the reduced capacitance resulting from shorter lead lengths. Finally, for scintillator readout the photodiodes must have good detection efficiency at the wavelengths of interest (400–500 nm).

II. Background

The starting point for the technology development is a phosphorus-doped, polycrystalline-silicon gettering technique originally used for high-energy physics detectors [4]. This work focuses on the modifications necessary in order for this process to yield back-illuminated photodiodes with good blue/UV response given the wavelengths of light produced by scintillators of interest for PET, e.g. bismuth germanate (BGO) with $\lambda = 480$ nm and cerium-doped lutetium orthosilicate (LSO) with $\lambda = 415$ nm.

Due to the strong absorption of short wavelength light in silicon [5], an optically transparent contact layer must be developed in order for back illumination to be viable. For example, at $\lambda = 400$ nm the absorption length in silicon is 0.1–0.2 μm, where absorption length is the inverse of absorption coefficient, and is the depth at which the light intensity is $1/e \approx 37\%$ of the original incident intensity. The back-side layer used for gettering in the original process [4] is much too thick (1 μm) to allow transmission of the short wavelength light of interest in the PET application. Various techniques for forming an optically transparent contact window on the back side of the wafer were investigated. The requirements of this layer are that it be optically transparent while maintaining the low leakage currents characteristic of the polysilicon gettering process. In addition, the layer should not add appreciably to the series resistance and hence the noise.

Back and front-illuminated photodiodes and radiation detectors with ion implanted p^+ junctions have been reported [6, 7, 8], and implantation of the back-side contact was considered for these devices. For a thin n^+ layer, the preferred n-type species would be arsenic, due to its large atomic mass and hence small implant range in silicon [9]. However, based on previous results [4] there were concerns that the leakage current would increase as a result of the high-temperature anneals required to activate the dopants and remove the implant damage.

There have also been reports of blue/UV sensitive photodiodes using diffused contacts [10, 11, 12]. For n-type impurities (phosphorus and arsenic), dopant pile up near the silicon-silicon dioxide interface results in a built-in field which enhances the separation of the photogenerated electron-hole pairs and therefore increases the quantum efficiency. With careful processing a recombination-free layer can result when

[1]This work supported in part by the U.S. Department of Energy under Contract DE-AC-76SF00098, and in part by the National Institutes of Health under grants P01-HL25840 and R01-NS29655.

the doping level is maintained below the value where Auger recombination is significant. We have not investigated this technique due to concerns that high-temperature diffusion steps may result in increased leakage current.

Other more exotic techniques such as molecular beam epitaxy [13], molecular layer doping [14], or gas immersion layer doping [15] were ruled out because of concerns about expense and lack of readily available fabrication equipment. However, these techniques offer great promise for future development.

III. Device Design

The technique we have selected for fabricating the optically transparent back-side window involves etching the thick polysilicon gettering layer near the end of the process and re-depositing a much thinner layer to serve as the n^+ blocking contact. By depositing a series of contact layers with varying thicknesses, we determined that this layer can be made as thin as 10 nm while maintaining low leakage currents.

A drawback to the use of polysilicon for the contact to be illuminated is that the optical absorption coefficient of doped polysilicon is larger than that of single-crystal silicon, e.g. heavily-doped polysilicon is about twice as absorbing as lightly-doped, single-crystal silicon [16]. However, the fact that the polysilicon can be made thin minimizes this drawback. In addition, the process required is simpler when compared to the more advanced techniques [13, 14, 15] and, as shown later, is compatible with the low leakage currents required for this application.

The silicon photodiode arrays were fabricated on 300 μm thick, high resistivity n-type silicon substrates. The resistivity was approximately 8,000 Ω-cm and the crystalline orientation was $\langle 100 \rangle$. The 3 mm square photodiodes were arranged in 3×4 arrays, with a guard ring around the periphery of the array. The photodiodes are operated fully depleted, which allows for minimal capacitance and back illumination since the electric field used to separate photogenerated electron-hole pairs extends to the back contact.

The quantum efficiency was measured by comparison to a photodiode with a known spectral response. A tungsten lamp was used for $\lambda = 400$–1100 nm, and a Hg vapor lamp was used for $\lambda = 300$–450 nm. The light passed through a monochromator and was focused on the test photodiode and the calibrated photodiode via optical fibers. Figure 1 shows the measured quantum efficiency versus wavelength for polysilicon thicknesses ranging from 100 nm to 10 nm. At longer wavelengths, the quantum efficiency is essentially equal to the quantum efficiency calculated by assuming only reflection loss due to the mismatch in the refractive indices of silicon and air (silicon refractive index ≈ 3.7). At shorter wavelengths, the loss of collected charge due to the absorption in the polysilicon contact causes the quantum efficiency to deviate from the reflection limit. Note that for the thinnest film (10 nm), the measured quantum efficiency is very close to the reflection limit; at $\lambda = 415$ nm, the reduction in quantum efficiency that can be attributed to loss in the polysilicon layer is $\approx 6\%$.

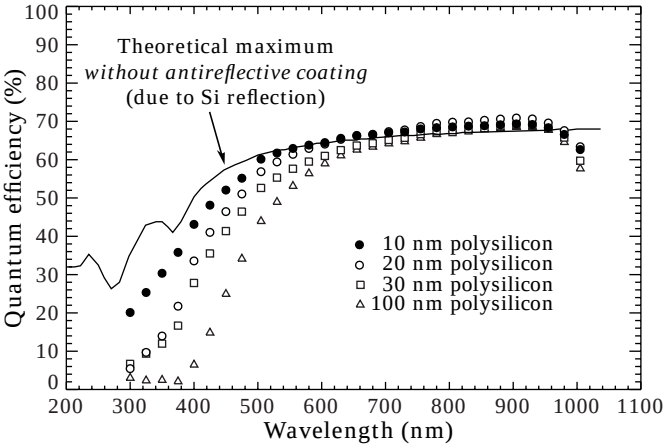

Fig. 1 Quantum efficiency versus wavelength for varying polysilicon thicknesses. The results are for 300 μm thick p-i-n photodiodes.

The quantum efficiency can be improved beyond the reflection limit by the addition of an antireflection (AR) coating. We initially investigated AR coatings of SiO_2, but have focused our attention on indium tin oxide (ITO), which has several advantages for this application.

ITO films can have transmittances exceeding 80% over a broad spectral range [17], and the refractive index of ITO (≈ 1.8–2.2) is a good match to silicon. Zero reflection at normal incidence can theoretically be obtained when the refractive index value is the geometric mean between that of air and silicon [18]. Since the film can be deposited at low temperatures the process is not expected to degrade the leakage current of the photodiodes. In addition, ITO is electrically conducting and therefore can simultaneously act as an AR coating and reduce the resistance of the thin back-side layer and its associated noise. High resistance in the back-side contact is a concern with all of the previously mentioned techniques used to make thin layers, and the problem is exacerbated for large arrays where the physical contact may be located a significant distance from the detecting element.

IV. Development of ITO AR coating

The ITO layers were deposited at room temperature by RF magnetron sputtering from a target composed of 90 wt.% In_2O_3 and 10 wt.% SnO_2 (target area 12 cm by 38 cm). The power used for all depositions was 500 W. The conduction in ITO is due to oxygen vacancies, and therefore the oxygen concentration in the film must be well controlled. Based on deposition parameters reported in Ref. 19, the films were reactively sputtered in a mixture of O_2 and Ar. The total sputter pressure was varied from 2–8 mTorr and the O_2 concentration was varied from 0–5% in order to determine deposition conditions that would yield films with low resistivity and high optical transmittance.

In order to take into account both the resistivity and the transmittance in evaluating the quality of the films, the thickness-independent quantity, $R_\square \ln(1/t)$, was used as a figure of merit, where $R_\square$ is the sheet resistance and t is the optical transmittance at a given wavelength. The sheet resistance of the films was measured using a four-point probe,

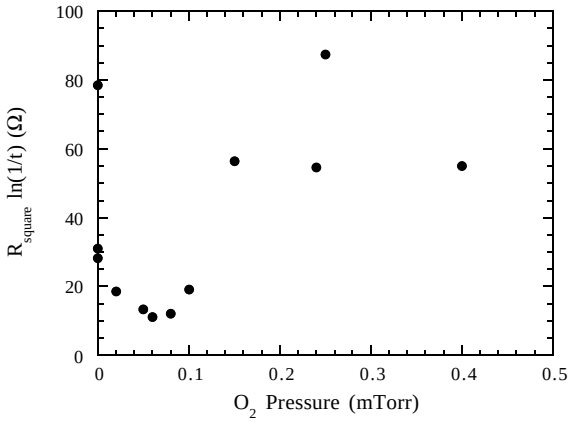

Fig. 2 Figure of merit for ITO films plotted versus oxygen partial pressure during film deposition. $R_\square$ is the film sheet resistance, and t is the transmittance at a wavelength of 800 nm.

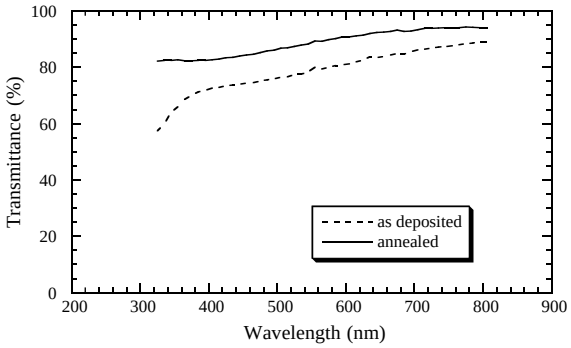

Fig. 3 Transmittance versus wavelength for an ITO film deposited on glass. The anneal was 1 hour at 200°C in nitrogen and the film thickness was 54.5 nm.

and the optical transmittance was measured using a dual-beam spectrophotometer with a tungsten halogen lamp. Plotted as a function of O_2 partial pressure during film deposition, $R_\square \ln(1/t)$ exhibits a noticeable minimum; as shown in Figure 2, the best films result at O_2 partial pressures of 0.04–0.08 mTorr.

For the back contact to the photodiode arrays, ITO was deposited at a total pressure of 2 mTorr and an O_2 partial pressure of 0.06 mTorr. At these deposition conditions, the films exhibited resistivities of $\approx 4.8\times10^{-4}\,\Omega$-cm. A low temperature, post-deposition anneal further improved the quality of the films: a one hour anneal at 200°C in N_2 lowered the resistivity to $\approx 3.4\times10^{-4}\,\Omega$-cm. Hall effect measurements on an ITO sample before and after annealing showed that the carrier density increased from 6.7×10^{20} cm^{-3} to 8.7×10^{20} cm^{-3} and that the carrier mobility changed slightly, from 19 cm^2/V-sec to 21 cm^2/V-sec. The anneal also increased the transmittance of the film, as shown in Figure 3 for a 54.5 nm-thick film. The transmittance particularly increased at wavelengths just below 400 nm, perhaps indicating an increase in the energy gap of the material. The transmittance at $\lambda = 415$ nm, the wavelength at peak emission for LSO, increased from 73% to 83%.

The thickness of the ITO AR coating can be chosen so that it minimizes reflection by acting as a quarter-wave plate for the

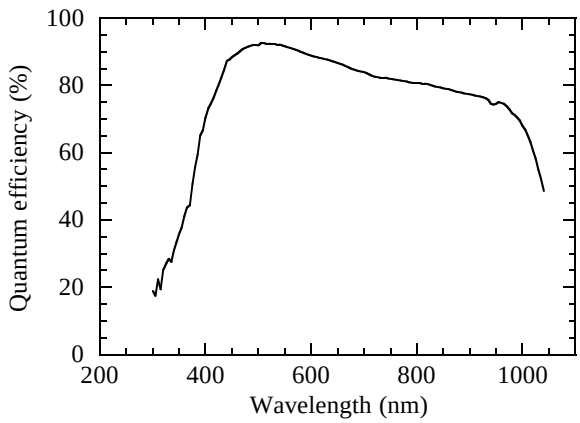

Fig. 4 Measured quantum efficiency versus wavelength for a back-illuminated, 300 μm thick p-i-n photodiode. The polysilicon thickness was 10 nm, and the ITO thickness was 57 nm.

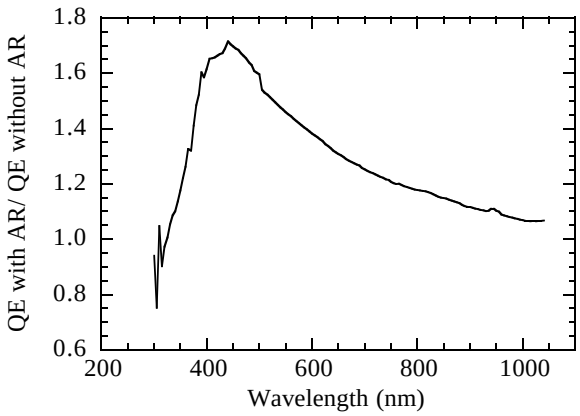

Fig. 5 Ratio of measured quantum efficiency with and without the ITO AR coating versus wavelength for the photodiode of Figure 4.

wavelength of interest, i.e.

$$X_{ITO} = \frac{\lambda}{4n} \tag{1}$$

where X_{ITO} is the ITO film thickness that minimizes reflection at the wavelength λ, and n is the refractive index of ITO. Figure 4 shows the quantum efficiency versus wavelength for a back-illuminated photodiode with a 57 nm ITO layer deposited on a 10 nm polysilicon layer. The thickness was chosen to maximize the quantum efficiency at the LSO wavelength (415 nm). Figure 5 shows the ratio of the quantum efficiency of the photodiode with and without the AR coating. The improvement in quantum efficiency due to the AR coating exceeds 60% over a 100 nm wavelength range and peaks at $\lambda \approx 450$ nm, close to the target value. As shown in Figure 4, the combination of the thin polysilicon contact and quarter-wave ITO layer yields a quantum efficiency of approximately 75% at the LSO wavelength. For BGO, the quantum efficiency is even higher, $\approx$ 90% at 480 nm, and should be improved even further for a quarter-wave ITO thickness optimized for the BGO wavelength.

V. NOISE PERFORMANCE

Photodiodes were connected to readout amplifiers and noise characteristics were measured at room temperature. The dependence of equivalent input noise charge on photodiode and preamplifier characteristics is given by [20]

$$\begin{aligned} {Q_n}^2 &\propto \left(4kTR_S + {v_{eq}}^2\right){C_T}^2\tau^{-1} \quad Series \\ &\propto 2qI_D\tau \quad Parallel \\ &\propto A_F{C_T}^2 \quad 1/f \end{aligned} \tag{2}$$

where k is Boltzmann's constant, T is temperature in Kelvin, R_S is the series resistance of the photodiode plus leads, τ is the shaping time of the RC-CR shaping network, q is the electronic charge, I_D is the photodiode leakage current, and v_{eq} and A_F are the equivalent input noise voltage and $1/f$ coefficient of the preamplifier, respectively. C_T is the total capacitance at the input of the amplifier due to the photodiode, preamplifier and leads used to connect the diode to the preamplifier. Thus, the photodiode properties that affect the noise are the capacitance, the series resistance, and the leakage current, although some care must be taken in materials selection to avoid increasing the A_F factor.

The capacitance of the photodiode for a given area, set by the size of the scintillator crystals, is reduced by using thick devices ($\approx 300\ \mu$m). The two additional photodiode parameters that must be minimized for the best noise performance are the leakage current and series resistance. The ITO layer on the n-side and the Al coating on the p-type contacts reduce the series resistance, and as mentioned previously, the polysilicon gettering process yields low leakage currents. Figure 6 shows a typical measured leakage current for one of the photodiodes in the 3 × 4 array. The polysilicon back-side layer is 10 nm thick and the ITO AR coating is 57 nm thick. The leakage current at 100V bias voltage is about 0.3 nA/cm^2. Also shown in Figure 6 is the measured photodiode capacitance versus bias voltage. The substrate doping density extracted from the C-V measurements is approximately 4-6 × 10^{11} cm^{-3} and the depletion voltage is approximately 30V.

The detector noise was evaluated by connecting a pixel of the array to the input of an amplifier channel of the IC described in Ref. 3 and measuring the noise at room temperature as a function of shaping time. Note that this amplifier uses a compensating current as opposed to a large value resistor to sink the detector leakage current, which multiplies the noise due to leakage current by $\sqrt{2}$ over the value given in equation (2). Figure 7 shows the measured noise from three pixels from different locations in the array and on different arrays as well as from a CK-05 capacitor with similar capacitance. The amplitude of the test input pulse was $\approx 2400\ e^-$, similar to the expected signal from the LSO crystals.

The noise data with the capacitor characterize the amplifier performance and indicate the noise obtainable with an "ideal" photodiode, that is, a photodiode with capacitance but no series resistance, leakage current, or $1/f$ noise. All three pixels have similar noise properties and compare well with the "ideal photodiode" curve. The increase over the "ideal" curve at longer shaping times is consistent with the contribution due to the non-zero leakage current, while the increase at short shaping times is likely to be due to a small series resistance. The minimum noise level is typically 140 e^- rms, obtained with a 3-4 μs shaping time.

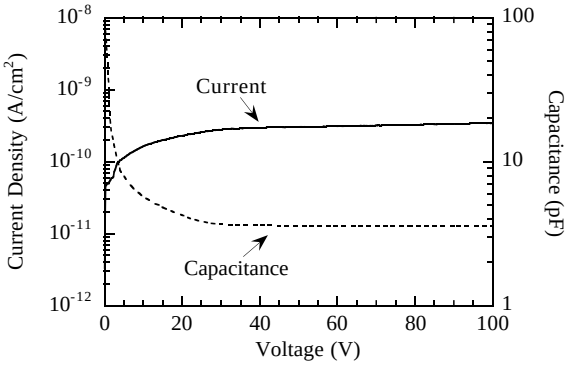

Fig. 6 Leakage current and junction capacitance measured on a 3 mm × 3 mm photodiode that is part of a 3 × 4 array. The thicknesses of the back-side polysilicon and ITO were 10 nm and 57 nm, respectively. The surrounding pixels were connected to a guard ring that was biased at the same voltage as the pixel being tested.

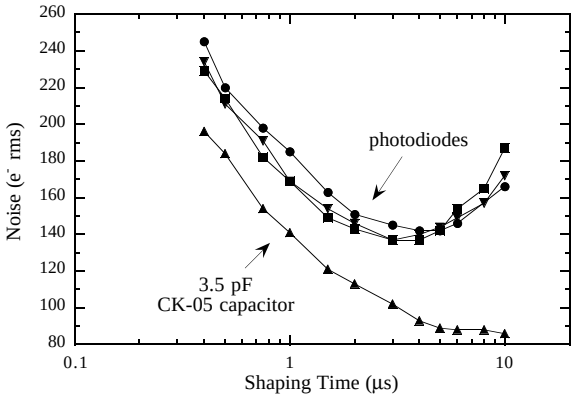

Fig. 7 Noise versus shaping time for 3 mm × 3 mm photodiodes as described in Figure 6. One photodiode was connected to an amplifier channel (Ref. 3) with the remaining photodiodes and guard ring biased at the same potential as the amplifier input.

The ability to accurately measure gamma ray energies was tested by coupling one element of the photodiode array with optical grease to a 3 mm diameter, 5 mm tall cylinder of CsI(Tl) scintillator coated with Teflon tape reflector. CsI(Tl) has a light output of 52,000 photons/MeV, with a peak emission wavelength of 535 nm and major decay time components of 700 ns (66% of the emitted light) and 3.3 μs (34%). The scintillator was excited at room temperature with 141 keV gamma rays from ^{99m}Tc, and the photodiode output was amplified with a 10 μs shaping time using the same charge sensitive amplifier as above.

The resulting pulse height spectrum, plotted in Figure 8, shows a clear photopeak with a 12% fwhm energy resolution. This resolution is significantly better than the 19% that is typically obtained with cooled silicon photodiodes [21] and comparable to the 9.4-12% obtained with high band gap photodetectors such as HgI_2 [22, 23], largely due to the

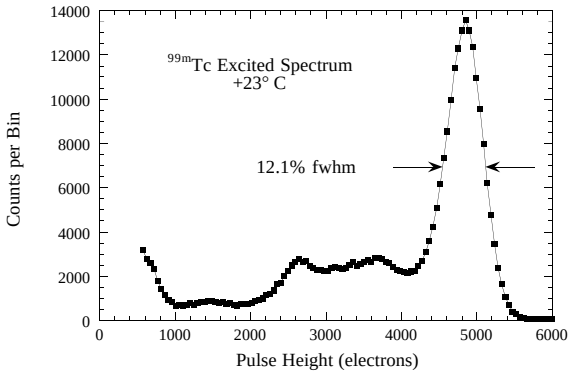

Fig. 8 Measured pulse height spectrum for a CsI(Tl) scintillator excited with 141 keV gamma rays from ^{99m}Tc.

combination of high quantum efficiency and low leakage current obtained with these photodiodes.

VI. Conclusions

A back-illuminated photodiode technology has been described. Signal-to-noise ratio is maximized by the development of high quantum efficiency photodiodes with low leakage current and low series resistance. The high quantum efficiency at short wavelengths results from the use of a thin (10 nm) back-side polysilicon contact in conjunction with a 57 nm ITO antireflection coating. The noise is reduced due to the low leakage current possible with this process and to the low series resistance that the ITO provides to the back-side contact. For devices optimized for detection of scintillation light produced by LSO, the quantum efficiency is 75% and the noise level is 140 e^- rms, measured at room temperature.

VII. Acknowledgements

We would like to thank N. Palaio for his assistance in developing the ITO process, D. Groom for his advice regarding the QE measurement, M. Ho for automating the transmission measurement, and G. Gruber for performing the noise measurements.

This work is supported in part by the Director, Office of Energy Research, Office of Health and Environmental Research, Medical Applications and Biophysical Research Division of the U.S. Department of Energy under contract No. DE-AC03-76SF00098, and in part by the Public Health Service grants No. P01-HL25840 and No. R01-NS29655, awarded by the National Heart, Lung, and Blood Institute, and the Neurological Disorder and Stroke Institute, Department of Health and Human Services.

VIII. References

[1] W.W. Moses and S.E. Derenzo, "Design studies for a PET detector module using a pin photodiode to measure depth of interaction," IEEE Trans. Nucl. Sci., **41**, 4, 1441-1445, August 1994.

[2] W.W. Moses, S.E. Derenzo, C.L. Melcher, and R.A. Manente, "A room temperature LSO/pin photodiode PET detector module that measures depth of interaction," IEEE Trans. Nucl. Sci., **42**, 4, 1085-1089, August 1995.

[3] W.W. Moses, I. Kipnis, and M.H. Ho, "A 16-channel charge sensitive amplifier IC for a PIN photodiode array based PET detector module," IEEE Trans. Nucl. Sci., **41**, 4, 1469-1472, August 1994.

[4] S. Holland, "Fabrication of detectors and transistors on high-resistivity silicon," Nuclear Instrum. Methods in Physics Research, **A275**, 537-541, 1989.

[5] S. M. Sze, *Physics of Semiconductor Devices*, 2nd Edition, p. 750, Wiley, 1981.

[6] T.-E. Hansen, "Silicon detectors for the UV- and blue spectral regions with possible use as particle detectors," Nuclear Instrum. Methods in Physics Research, **A235**, 249-253, 1985.

[7] T. Maisch, R. Günzler, M. Weiser, S. Kalbitzer, W. Welser, and J. Kemmer, "Ion-implanted Si pn-junction detectors with ultrathin windows," Nuclear Instrum. Methods in Physics Research, **A288**, 19-23, 1990.

[8] R. Hartmann et al, "Low energy response of silicon pn-junction detector," Nuclear Instrum. Methods in Physics Research, **A377**, 191-196, 1996.

[9] S. Wolf and R.N. Tauber, *Silicon Processing for the VLSI Era, Volume 1-Process Technology*, p. 290, Lattice Press, 1986.

[10] K.W. Wenzel, C.K. Li, D.A. Pappas, and R. Korde, "Soft X-ray silicon photodiodes with 100% quantum efficiency," IEEE Trans. Nucl. Sci., **41**, 4, 979-983, August 1994.

[11] R. Korde and J. Geist, "Quantum efficiency stability of silicon photodiodes," Applied Optics, **26**, 24, 5284-5290, December 1987.

[12] R. Korde and J. Geist, "Stable, high quantum efficiency, UV-enhanced silicon photodiodes by arsenic diffusion," Solid-State Electronics, **30**, 1, 89-92, January 1987.

[13] M.E. Hoenk, P.J. Grunthaner, F.J. Grunthaner, R.W. Terhune, M. Fattahi, and H.-F. Tseng, "Growth of a delta-doped silicon layer by molecular beam epitaxy on a charge-coupled device for reflection-limited ultraviolet quantum efficiency," Appl. Phys. Lett., **61**, 9, 1084-1086, August 1992.

[14] Y. Saitoh et al, "New profiled silicon PIN photodiode for scintillation detection," IEEE Trans. Nucl. Sci., **42**, 4, 345-350, August 1995.

[15] P.G. Carey, K. Bezjian, T.W. Sigmon, P. Gildea, and T.J. Magee, "Fabrication of submicrometer MOSFET's using gas immersion laser doping (GILD)," IEEE Elec. Dev. Lett., **7**, 7, 440-442, July 1986.

[16] G. Lubberts, B.C. Burkey, F. Moser, and E.A. Trabka, "Optical properties of phosphorus-doped polycrystalline silicon layers," Journal of Applied Physics, **52**, 11, 6870-6878, November 1981.

[17] D.K. Schroder, "Transparent gate silicon photodetectors," IEEE Trans. Elec. Dev., **25**, 2, 90-97, Feb. 1978.

[18] O.S. Heavens, *Optical Properties of Thin Solid Films*, p. 209, Dover, 1991.

[19] S.B. Lee, J.C. Pincenti, A. Cocco, and D.L. Naylor, "Electronic and optical properties of room temperature sputter deposited indium tin oxide," Journal of Vacuum Sci. and Tech., **A11**, 5, 2742-2746, September/October 1993.

[20] V. Radeka, "Low-noise techniques in detectors," Ann. Rev. Nucl. Part. Sci., **38**, 217-277, 1988.

[21] A.J. Bird, T. Carter, A.J. Dean, D. Ramsden, and B.M. Swinyard, "The optimisation of small CsI(Tl) gamma-ray detectors," IEEE Trans. Nucl. Sci., **40**, 4, 395-399, August 1993.

[22] Y.J. Wang, B.E. Patt, J.S. Iwanczyk, S.R. Cherry, and Y. Shao, "High efficiency CsI(Tl)/HgI_2 gamma ray spectrometers," IEEE Trans. Nucl. Sci., **42**, 4, 601-605, August 1995.

[23] B.E. Patt et al, "Mercuric iodide photodetector arrays for gamma-ray imaging," Nuclear Instrum. Methods in Physics Research, **A380**, 295-300, 1996.